Proceedings of ICEME 2001

Highly Dielectric Strength of N_2/solid Composite Insulating System under Nonuniform Field

Hideki Ueno and Hiroshi Nakayama
Department of Electrical Engineering, Faculty of Engineering
Himeji Institute of Technology
2167 Shosha, Himeji 671-2201, Japan
Tel:+81-792-67-4863, Fax:+81-792-67-4855
E-mail: ueno@elct.eng.himeji-tech.ac.jp

SF_6 gas has excellent dielectric insulating properties, and has contributed to the improvement of the reliability and miniaturization of the electric power apparatuses such as a GIS [1]. However, a significant decrease of dielectric strength is induced under a nonuniform electric field by the existence of a protrusion on the conductor or a metallic impurity, or by invasion of a steep front surge [2]. Moreover, recently the leakage of SF_6 is regulated like CO_2, because the ability of contribution to greenhouse effect is very high compared with that of CO_2 [3]. N_2/SF_6 mixed gas and high pressure N_2 gas have been very interested in the practical application as an insulating medium in place of SF_6 [4]. However, the dielectric insulation characteristics of N_2/SF_6 mixed gas under the nonuniform field have not been clarified. Especially, dielectric insulating properties for the system with a small gap have not been elucidated. Because the dielectric breakdown process under the nonuniform field is very complicated by corona stabilization.

Now, an insulating configuration of the power apparatuses consists of a solid dielectric and an insulating gas, because of supporting the conductor or coating the electrode by the insulators. The creeping flashover characteristics for the composite insulation under the nonuniform field are very important from fundamental and practical points of view. The characteristics of the composite insulating system have been focused under the highly nonuniform field induced by a protrusion or a metal particle in the small gap in our previous report [4,5]. In this paper, we describe anomalous creeping flashover characteristics for the needle-plane configuration with a solid insulating barrier in the N_2/SF_6 mixture and discuss the behavior associated with the corona extension process depending on the barrier surface shape.

Figure 1 shows the electrode configuration for the present work. The gap was composed of a needle electrode with a tip of 35 μm radius of curvature and a 35 x 35 mm^2 plane electrode. The electrode distance d between a needle and a plane was adjusted at d=1.0 mm by a micrometer mounted on the needle electrode. A borosilicate glass insulating barrier (18 x 18 mm^2) with thickness a=1.0 mm was placed on the upper surface of the plane. The barrier with a groove of 20 μm in width and of 0.15 mm in depth, or with a 0.15 mm-step along the center axis of the surface was used. Above configuration was set up in a vessel and then was filled with N_2/SF_6 mixtures at P=0.1~0.3 MPa. A rectangular pulse voltage with a wavefront duration T_f=1.5 μs and a maximum peak value V_p=35 kV was applied.

Figure 2 shows the SF_6 gas content dependence of negative FOV and corona onset voltage (COV) for various barriers at d=2.0 mm under P=0.2 MPa. The reduction of the negative FOV was induced by the addition of 3% of SF_6. In our previous report [4], the SF_6 content dependence of negative creeping FOV has been strongly affected by the creeping distance and the gas pressure. In the present

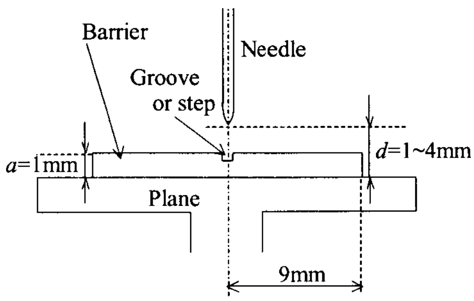

Fig.1 Electrode configuration.

work, we point out the effect of the barrier surface shape (flat, grooved and step). Namely, in the case of the barrier with flat surface and the barrier with 0.15mm-step along the center axis on the surface, a large decrease of negative FOV was observed by small SF_6 addition. In the case of the barrier with a groove (0.15 mm in depth and 20 μm in width), the negative FOV in N_2 (D=0%) was about 10 kV lower than those for the other barrier systems, so that the reduction of the negative FOV induced by 3% SF_6 addition was considerable small in comparison with those obtained for the flat barrier and the stepped barrier. These facts suggest that the decrease of negative FOV by the small SF_6 addition is strongly affected by the configuration such as gap length and creeping distance and gas pressure, but also by the barrier surface shape.

The reduction of the FOV upon the admixture of SF_6 gas has been also reported for N_2/SF_6 gas mixtures at a long nonuniform gap without a barrier by several reports [6,7]. Watanabe and Takuma reported that the decrease of the FOV was found in both polarities and was attributed to the weak corona stabilization [5]. The decrease of the FOV was induced by the insertion of the barrier between the needle electrode and the pressure dependence of FOV associated with the corona stabilization was not observed. Therefore, the present reduction of FOV should not be directly result in the contribution of the corona stabilization. Safar *et al.* interpreted by unique photon-related properties of N_2/SF_6 gas mixture [7]; however, the mechanism was not discussed in detail. Therefore, to clarify the reason why the reduction of negative FOV is induced by the small addition of SF_6 into N_2 is very important from fundamental and practical points of view.

The anomalous SF_6 gas content dependence of creeping FOV was observed for the negative needle, namely, the FOV was considerably decreased by only 3% SF_6 gas admixture compared with that for pure N_2 gas system (D=0%). However, upon further increasing SF_6 gas content D, the FOV increased linearly in the range of $3\%<D<100\%$. In the present investigation, the FOV in N_2 (D=0%) for the flat and stepped barriers was comparable to that in SF_6 (D=100%). Such a high FOV in N_2 (D=0%) and decrease of FOV could not be observed for our needle-plane small gap configuration without a barrier. It is well known that the FOV in N_2 (D=0%) is 1/2~1/3 times lower than that in SF_6 (D=100%) under the uniform field. This fact that the FOV in N_2 (D=0%) is as high as that in SF_6 (D=100%) is considered that it may be one of the important roles on the anomalous flashover behavior.

At first, we have investigated the creping flashover characteristics in N_2 (D=0%) and effect of the barrier surface. Electrode distance dependence of negative FOV for various barrier surfaces in N_2 (D=0%) under P=0.2 MPa is shown in Fig.3. The FOVs in N_2 (D=0%) were 21, 25 and 28 kV for the grooved, stepped and flat barriers, respectively. In the case of flat and stepped barriers, the FOV increased with increasing electrode distance in the range of $1< d <2$ mm, and beyond d >2 mm the FOV indicated almost a constant value of 32 kV. In addition, no significant difference in negative

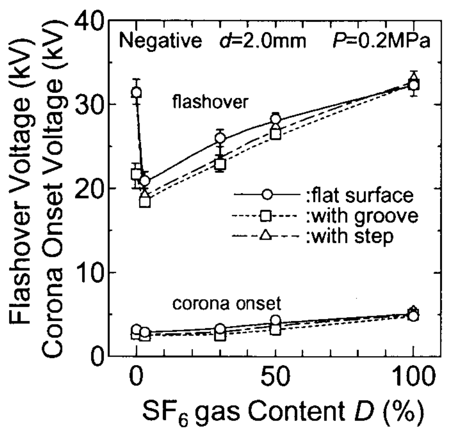

Fig.2 SF_6 content dependence of negative flashover voltage for various barrier surfaces.

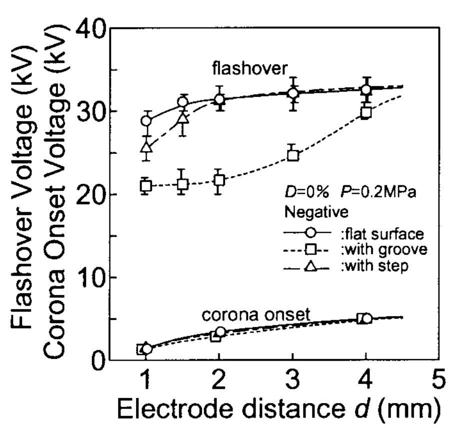

Fig.3 Electrode distance variation of negative flashover voltage for various barrier surfaces.

FOV between flat and stepped surfaces was found except for d=1.0 mm. In the case of the grooved surface, the FOV was not dependent of the electrode distance in the range of $1 < d < 2$ mm, and the FOV markedly increased with increasing d. By these differences in the electrode distance dependence of negative FOV, the FOV for the grooved surface was about 10kV lower than those for the flat and stepped surfaces. On the other side, though the COV increased with increasing d, and the value was almost same among three kinds of the barrier surface. It should be noted that the remarkable difference in negative FOV might result from the creeping corona extension process in N_2 (D=0%) depending n the barrier surface.

Corona extension images for the grooved barrier for d=2 mm under P=0.2 MPa are shown in Fig.4. In N_2 (D=0%), a wide and broad photon radiation on the barrier surface from the needle tip was observed and it became intense and exteneded by increasing applied voltage (Frame 2-3). And then, the clear and straight path was formed along the groove (Frame 4). On the other hand, corona extension in N_2/SF_6 (D=3%) was very different from that observed in N_2 (D=0%). In this case, the relative strong corona emission was found at the needle tip at lower voltage inspite of no difference on the corona onset voltage (Frame 2), and the corona extension on the barrier surface was suppressed (Frame 3). And then, the creeping corona developed with a very high speed along the groove (Frame 4). The similar observation has been performed for the stepped barrier system. For the stepped barrier system, the corona extension behavior was similar to that observed for the grooved barrier system, however, the corona extension for the grooved system, especially in N_2, was faster than that of the stepped barrier system.

From these observations, the anomalous creeping flashover charcteristics in N_2/SF_6 mixtures content variation of the negative FOV and its barrier surface effect are interpreted as follows and its scheme is shown in Fig.5. In the case of N_2 (D=0%) system, the corona from the needle is widely spread on the barrier and becomes gradually intense, so the negative charges by the corona are accumulated widely, therefore, the field relaxation is effectively resulting in the higher FOV. This interpretation is supported by the study on the accumulated charge by the dist figure method. Namely, the charges are accumulated widely on the barrier surface in N_2 (D=0%), on the other side, the charge accumulated area is defined locally just below and around the needle in N_2/SF_6 (D=3%). In the case of the grooved barrier, photons with higher energy (ultra-violet region) from the top of the streamer radiate to the barrier surface, and they are trapped and confined in the groove, so photoelectron emission nad photoionization can be activated in the groove, resulting in lower FOV.

On the contrary, in N_2/SF_6 (D=3%), the corona extension from the needle tip is suppressed by the negative ions generated by the electron attachment. At this time, the number of accumulated charges are little and the accumulated area is defined in comparison with the case of N_2 system, because the corona suppressed at the needle tip, so that the

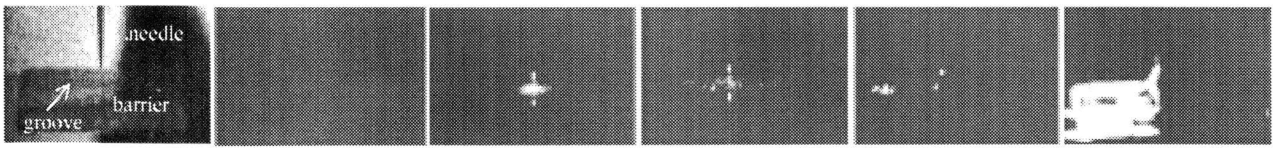

Configuration　Frame 1: 4.0 – 7.2kV　Frame 2: 7.7 – 11.2kV　Frame 3: 11.8 – 15.4kV　Frame 4: 15.8– 19.3kV　Frame 5: 19.8 – 23.3kV

(a) N_2 (D=0%)

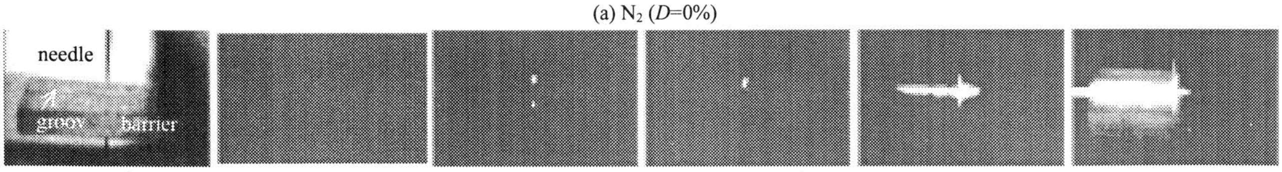

Configuration　Frame 1: 4.7 – 6.8kV　Frame 2: 7.0 – 9.9kV　Frame 3: 10.3 – 13.3kV　Frame 4: 13.8 – 16.6kV　Frame 5: 17.0 – 19.8kV

(b) N_2/SF_6 (D=3%)

Fig.4 Corona extension images in N_2 (D=0%) and N_2/SF_6 (D=3%) for the grooved barrier.

field relaxation effect by the accumulated charge should be weak. Furthermore, the electric field at the top of the streamer should be very high, therefore, the electrons might not always attach to SF_6 molecules and the SF_6^- can easily release the electron at low energy [8]. By this procedure, the electrons will be supplied in front of creeping corona. Then, at front of the creeping corona on the barrier surface, a large number of photons will be generated by recombination and relaxation of ionized or excited N_2 molecules. In addition, photoelectron emission from the barrier surface and release of the trapped electrons on the barrier surface would be induced by these photons. In particular, the photons will be absorbed effectively in N_2/SF_6 [9], and the ionization and the recombination will be activated in front of the streamer.

Creeping flashover characteristics has been investigated for composite insulating system consisted of insertion of the insulating barrier between the needle electrode and the plane electrode. The negative FOV for the flat and stepped systems in N_2 (D=0%) is as high as that of SF_6 (D=0%) by the effective field relaxation from the accumulated charges. Remarkable reduction of FOV induced by few percentages SF_6 addition should originate from the barrier interaction such as ineffective charge accumulation and photon-related emission. However, for the grooved system, the confinement effect should be effective, resulting in lower FOV in N_2.

REFERECES

[1] W.T.Shugg: "*Handbook of Electrical and Electronic Insulating Materials*", Second Edition (IEEE Press, NY, 1995).
[2] A.H.Cookson and O.Farish: IEEE Trans. PAS, 92, pp.871-876 (1973)
[3] L.Niemeyer and F.Y.Chu: IEEE Trans. EI, 27, pp.184-187 (1992).
[4] H.Ueno, N.Sakamoto and H.Nakayama: IEEE Trans. DEI, 8, pp.195-202 (2001).
[5] H.Ueno, Y.Egawa, F.Kamatani and H.Nakayama: Proc. 9th. International Symposium on Gaseous Dielectrics, No.66 (2001).
[6] T.Watanabe and T.Takuma: J. Appl. Phys., 48, pp.3281-3287 (1977).
[7] Y.A.Safar, N.H.Malik and A.H.Qureshi: IEEE Trans. EI, 17, pp.441-450 (1980).
[8] S.R.Hunter, J.G.Carter and L.G.Christophorou: J. Chem. Phys., 90, pp.4879-4891 (1989).
[9] D.T.A.Blair, N.M.MacLeod and J.S.Orr: Proc. 4th. Int. Conf. Gas Discharge, IEE London, pp.401-403 (1978).

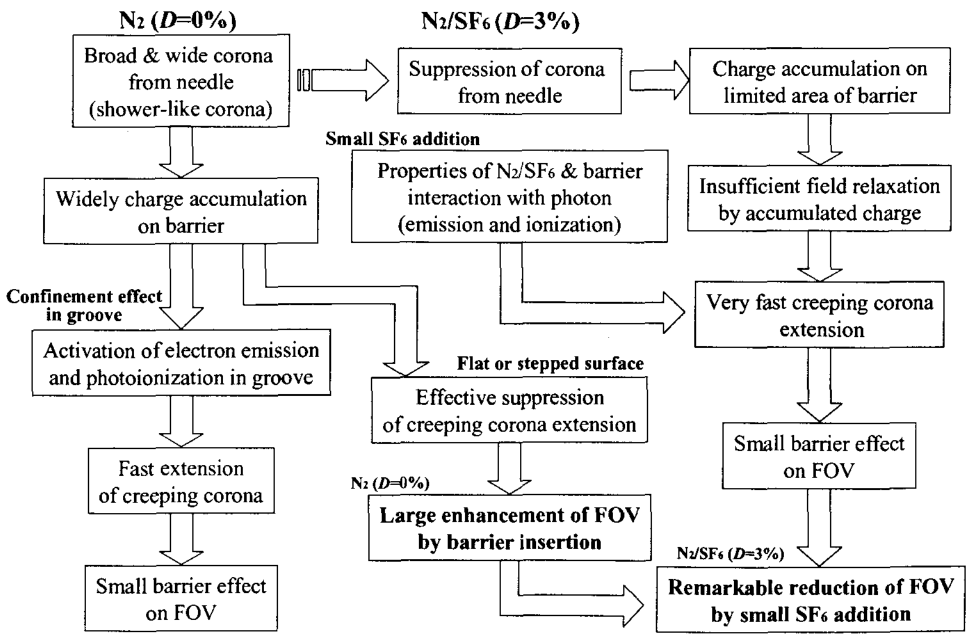

Fig.5 Scheme of creeping discharge characteristics for various barrier surfaces in N_2/SF_6 mixtures.